Australian Journal of Earth Sciences (2000) **47**, 1077–1085

Early Permian supra-subduction assemblage of the South Island terrane, Percy Isles, New England Fold Belt, Queensland

M. C. BRUCE AND Y. NIU

Department of Earth Sciences, University of Queensland, Qld 4072, Australia.

Ultramafic–intermediate rocks exposed on the South Island of the Percy Isles have been previously grouped into the ophiolitic Marlborough terrane of the northern New England Fold Belt. However, petrological, geochemical and geochronological data all suggest a different origin for the South Island rocks and a new terrane, the South Island terrane, is proposed. The South Island terrane rocks differ from ultramafic–mafic rocks of the Marlborough terrane not only in lithological association, but also in geochemical features and age. These data demonstrate that the South Island terrane is genetically unrelated to the Marlborough terrane but developed in a supra-subduction zone environment probably associated with an Early Permian oceanic arc. There is, however, a correlation between the South Island terrane rocks and intrusive units of the Marlborough ophiolite. This indicates that the two terranes were in relative proximity to one another during Early Permian times. A K/Ar age of 277 ± 7 Ma on a cumulative amphibole-rich diorite from the South Island terrane suggests possible affinities with the Gympie and Berserker terranes of the northern New England Fold Belt.

KEY WORDS: geochemistry, geochronology, Percy Isles, Permian, petrology, South Island terrane, supra-subduction zone.

INTRODUCTION

The South Island of the Percy Isles is located offshore from central Queensland (Figures 1, 2). It has been interpreted as originally being an integral part of the onshore Marlborough terrane of the northern New England Fold Belt (Figure 1). Its present-day dislocation was thought to result from dextral strike-slip displacement along the Stanage Fault Zone (Leitch *et al*. 1994; Morand 1997). This interpretation is based largely on the apparent lithological similarities. The South Island of the Percy Isles is dominated by serpentinised ultramafic rocks, as is the case in the Marlborough terrane. Leitch *et al*. (1994) described the South Island ultramafic association and termed this association the Northumberland Serpentinite and the Chase Point Metabasalt (revised here to the Chase Point Meta-andesite). However, little was known about the petrology and geochemistry of these rocks.

In this paper, we use new data to test whether or not rocks from South Island are related to the Neoproterozoic oceanic remnants of the Marlborough terrane (Bruce *et al*. 2000). The test indicates that the South Island rocks are genetically unrelated to the Marlborough terrane, and formed in a much younger supra-subduction zone environment. A new terrane, the South Island terrane, is suggested for these rocks. Recognition of this terrane provides a new perspective of the Permian development of the northern New England Fold Belt and points to possible links between the South Island, Gympie and Berserker terranes. The Stanage Fault Zone probably did displace rocks of the South Island and Marlborough terranes, however, these rocks were never part of the same assemblage.

PETROLOGY

The South Island terrane comprises an ophiolitic-type association of serpentinised ultramafic rocks, intermediate volcanics and granitoids interrupted by a sinistral strike-slip shear zone (R. J. Holcombe pers. comm. 1997), although Leitch *et al*. (1994) maintain that shear-sense indicators are dominantly dextral. This is the South Island Shear Zone of Leitch *et al*. (1994) that separates pillow lavas of the Chase Point Metabasalt (revised here to meta-andesite) and the Northumberland Serpentinite. Detailed analytical conditions for minerals are provided in Bruce *et al*. (2000).

Northumberland Serpentinite

Peridotites of the South Island terrane have experienced complete serpentinisation. The serpentinites have a massive texture, equigranular appearance and are blue-grey in colour. Glassy green serpentine flakes approximately 2 mm long are ubiquitous, as are small fibrous veins of chrysotile. Most samples studied are unweathered and remarkably fresh with no evidence of fracturing or veining.

These rocks show prograde, non-pseudomorphic textures of interpenetrating laths of antigorite usually embedded in serpentine of low birefringence. Serrate veins of chrysotile are also present. The antigorite blades are locally replaced by equant to slightly elongated metamorphic olivine and associated talc. Pyroxene bastites are not readily observed, but are probably represented by grains of differently orientated and/or ribboned serpentine. Magnetite also occurs as small veins and fine-grained aggregates as a result of serpentinisation.

Spherical crystals of chlorite are abundant throughout the rocks. Two types of relict chrome spinel are present with one type largely unaltered and the other altered to 'ferro-chrome' compositions. Unaltered chromium spinel has Cr# [Cr/(Cr + Al)] = 0.79 – 0.86, similar to spinels from peridotites dredged from the modern Mariana forearc (Bloomer *et al*. 1995) (Figure 3). They are, however, more Fe-rich and plot along the same trend as the Mariana peridotites. The spinels are also high in ferric iron (Table 1) (the locations of all samples mentioned in the tables are given in Appendix 1) suggesting formation under a relatively high oxygen fugacity. These observations are consistent with a supra-subduction zone origin (Parkinson & Pearce 1998).

Chase Point Meta-andesite

A fault zone consisting largely of metasedimentary rocks separates pillow lavas of andesite composition from serpentinite. The pillows are 0.5–1 m in diameter and are subrounded to elongated. They are greenish-grey in colour, fine grained and equigranular with a devitrified glassy rim commonly less than 1 cm thick. Black hornblende needles are embedded in the matrix. The pillows have been metamorphosed to low-grade greenschist facies.

In thin-section, the andesites display hornblende crystals embedded in a groundmass of plagioclase, mostly microlites and more rarely laths. Slight chloritic alteration of the feldspar is apparent. Veins of chlorite also cross-cut the groundmass in places. Hornblende crystals range from subhedral to acicular, usually < 1 mm in length. Fibrous actinolite has partially replaced hornblende in the majority of crystals.

Andesitic lavas lacking pillow structure also occur in structural contact with the serpentinite separated from the pillow lavas by rocks of the South Island Shear Zone. Small, black amphibole crystals occur in a greyish white groundmass. Chlorite veins cross-cut these samples. Petrography reveals the same basic mineralogy as the pillow lavas.

Meta-intrusive rocks

Medium-grained diorite and coarse-grained amphibole-rich diorite occur topographically below andesitic lavas in structural contact with the serpentinite. Field relations suggest that these coarser grained rocks are cumulative equivalents of the lavas, similar to crystal settling in a layered magma chamber. This interpretation is also consistent with their geochemistry (Table 2; Figure 4). The diorite is composed of primary hornblende phenocrysts and relict clinopyroxene crystals altered to varying extents to hornblende/actinolite and partially pseudomorphed by epidote. Plagioclase crystals have been saussuritised and replaced by chlorite. Metamorphic quartz and stilpnomelane are minor accessory minerals. The amphibole-rich diorite is composed of primary euhedral to subhedral magnesio-hastingsite crystals (4–6 mm), albitic plagioclase and relict accessory clinopyroxene. Clinopyroxene is partially to completely pseudomorphed by epidote. Relict chromium spinel is present and has a range of Cr# from

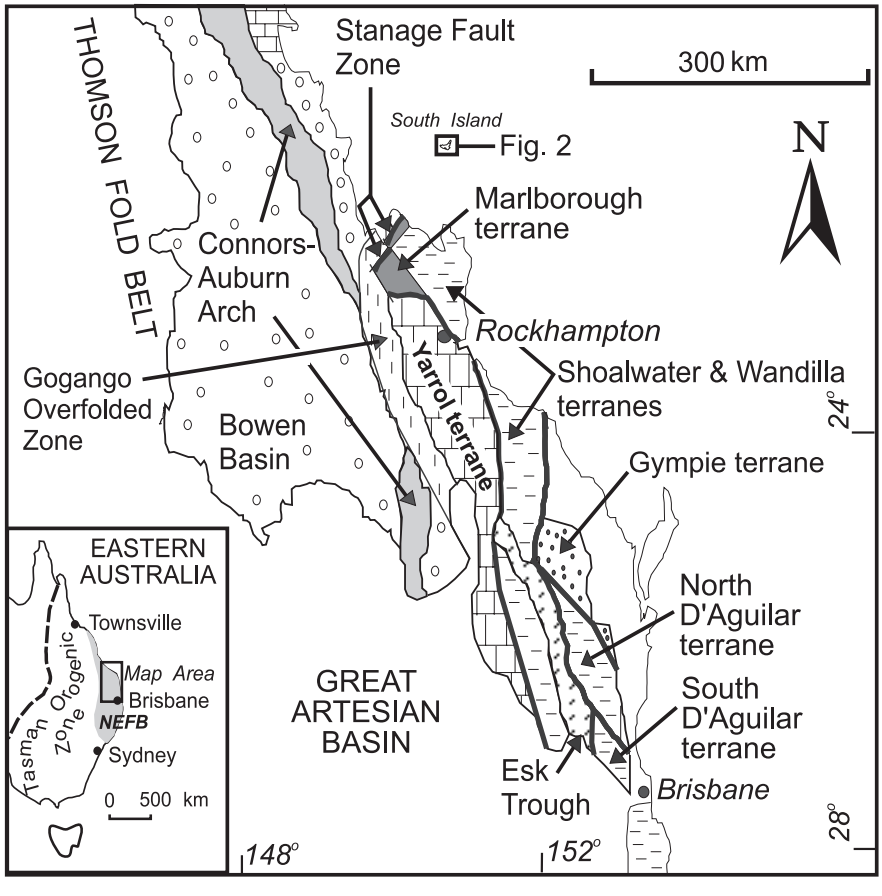

Figure 1 Major geological terranes of the northern New England Fold Belt. Note the location of the South Island, Percy Isles (Figure 2) and the onshore Stanage Fault Zone at the northern edge of the Marlborough terrane. Inset indicates the map area location within the New England Fold Belt (NEFB) of eastern Australia.

0.61 to 0.65 with variable Mg/Fe^{2+} ratios possibly due to MgO loss. Cr# > 0.60 are typical of volcanic arc rocks (Dick & Bullen 1984).

There are also diorite, granodiorite/tonalite dykes on South Island that show intrusive contacts with the Chase Point Meta-andesite. The diorite dykes consist of clinopyroxene crystals (largely altered to epidote) and hornblende crystals in a matrix of chloritised plagioclase, actinolite, prehnite/pumpellyite, epidote and chlorite. The granodiorite/tonalite dykes are finer grained, equigranular and composed predominantly of plagioclase and quartz with minor tremolite, actinolite and epidote as secondary minerals.

GEOCHEMISTRY

Analyses of representative samples are given in Table 2. Major elements for ultramafic rocks were determined by X-ray fluorescence (XRF) on a Phillips PW1400 at the University of Queensland. Major element analyses on other rocks were performed on a Varian Liberty 200 Inductively Coupled Plasma-Atomic Emission Spectrometer (ICP-AES) at Queensland University of Technology. Trace elements for all rocks were determined on a Fisons VG PlasmaQuad 2 Inductively coupled Mass Spectrometer at the University of Queensland following the procedure described by Niu and Batiza (1997).

Serpentinite

Chondrite normalised rare-earth element (REE) and primitive-mantle normalised multi-element plots for a representative harzburgite from the South Island terrane are presented in Figure 5. The South Island harzburgite is extremely depleted in REE with heavy-REE (HREE) concentrations ranging from 0.1 to 0.2-fold chondrite, middle-REE concentrations less than 0.07 to 0.005-fold chondrite, and light-REE (LREE) concentrations between 0.006 and 0.01-fold chondrite. The depleted nature of the LREE is consistent with residual harzburgite depleted by high degree melting as suggested by the occurrence of refractory chromium spinel in these samples. The broad REE similarities between the South Island harzburgite and harzburgites from the Torishima Forearc Seamount of the Izu Bonin oceanic arc (Parkinson & Pearce 1998) (Figure 5) further corroborate a supra-subduction zone origin of the South Island harzburgites. Enrichment in some LREE, and

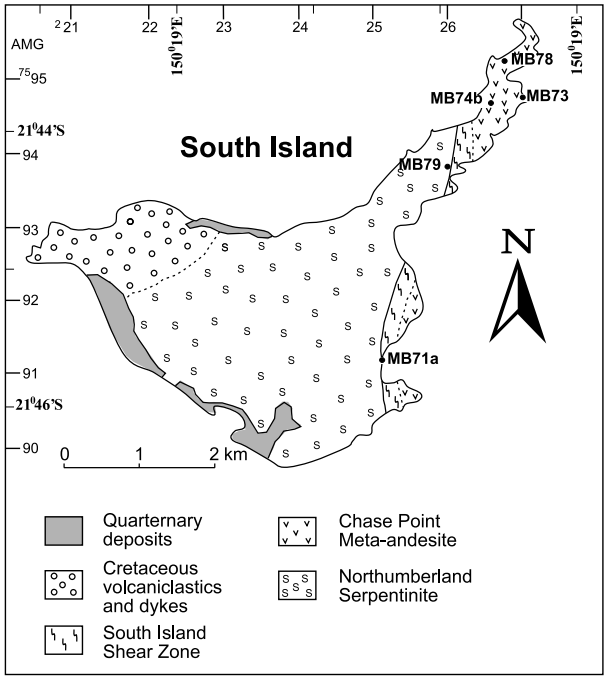

Figure 2 Simplified geological map of South Island (after Leitch *et al.* 1994). The South Island terrane comprises all units except the Cretaceous and Quaternary deposits. Coordinates are from the Percy Isles 1:100 000 topographic map (8954). Locations of samples listed in Table 2 are also shown.

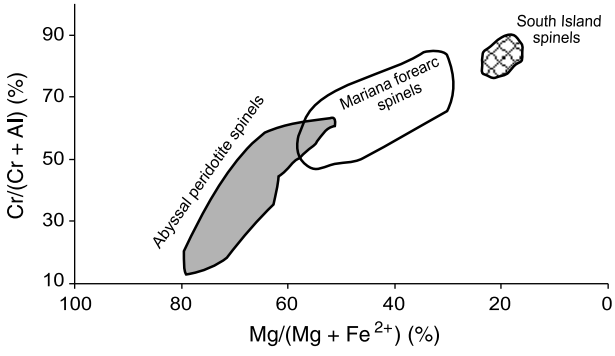

Figure 3 Plot of $Cr/(Cr + Al)$ *vs* $Mg/(Mg + Fe^{2+})$ compositions for spinels from the South Island harzburgites. Field of abyssal peridotite spinels after Dick and Bullen (1984); field of Mariana forearc spinels from harzburgite after Bloomer *et al.* (1995).

Table 1 Representative microprobe analyses of chromium spinel.

	MB71b Harzburgite	MB71c Harzburgite
SiO_2	0.00	0.09
TiO_2	0.09	0.21
Al_2O_3	6.06	7.39
Cr_2O_3	48.23	48.53
Fe_2O_3[a]	11.70	9.97
FeO[a]	28.22	27.81
MnO	1.05	0.86
MgO	3.76	4.11
Na_2O	0.01	0.00
K_2O	0.01	0.00
NiO	0.11	0.07
CaO	0.00	0.00
Total	99.23	99.03
Ions on the basis of 4 oxygen		
Ti	0.0024	0.0057
Al	0.2572	0.3105
Fe^{3+} [a]	0.3169	0.2676
Cr	1.3725	1.3684
Fe^{2+} [a]	0.8495	0.8294
Mg	0.2015	0.2185
Total	3.0000	3.0000
Cr#	0.84	0.82
Mg#	0.19	0.21

[a]Calculated from stoichiometry.
Cr# = Cr/(Cr + Al), Mg# = $Mg/(Mg + Fe^{2+})$.

in particular elements, such as Rb, Ba, U, and Sr, is consistent with refertilisation from a subducting-slab-derived fluid. However, the mobile nature of these latter elements could be associated with serpentinisation. The extreme fractionation of Nb from Ta (Nb/Ta = 3.6, significantly less than the chondritic ratio of 16–18) is consistent with the harzburgites being highly depleted residues (Niu & Hékinian 1997). The slight positive Eu anomaly (Figure 5) could be due to its mobility during serpentinisation or inherited from a fertile mantle source.

Table 2 Major and trace-element analyses of South Island terrane lithologies.

	MB71a Harzburgite GR251912	MB73 Diorite/Tonalite (adakite) GR270948	MB74b Tonalite (adakite) GR266947	MB78 Andesite GR268953	MB79 Diorite GR260939
SiO_2	38.59	56.04	62.86	55.73	46.86
TiO_2	0.01	0.40	0.25	0.60	0.69
Al_2O_3	0.75	16.22	17.90	16.13	11.37
Fe_2O_3*	7.26	4.94	3.28	5.96	10.27
MnO	0.10	0.10	0.07	0.10	0.17
MgO	40.20	7.33	2.78	5.22	17.22
CaO	0.55	6.23	6.21	5.95	9.62
Na_2O	0.21	5.86	4.71	6.97	2.09
K_2O	0.00	0.60	1.60	0.23	0.17
P_2O_5	0.00	0.28	0.06	0.07	0.03
LOI	12.05	1.22	1.25	2.89	3.11
Total	99.73	99.22	100.96	99.86	101.60
Li	0.16	6.49	5.84	4.33	10.06
Be	bd	0.87	0.76	0.45	0.23
Sc	8.76	20.24	9.79	19.95	40.19
Ti	32.15	nd	nd	nd	nd
V	40.8	137	65.7	123	195
Cr	3008	272	115.9	41.35	1378
Co	98.84	24.68	10.47	18.91	57.46
Ni	1875.35	90.81	11.83	5.44	385
Cu	3.86	27.28	16.73	9.98	44.93
Zn	37.13	40.13	32.61	34.47	78.20
Ga	0.79	16.47	17.34	11.44	10.51
Rb	0.10	10.57	29.13	3.18	1.29
Sr	2.75	176	406	572	62.69
Y	0.10	7.85	5.74	12.11	15
Zr	18.5	88.7	88.6	71.6	32.8
Nb	13.64	3.10	1.66	2.26	0.98
Cs	29.66	0.12	0.39	0.15	0.10
Ba	119	90.9	275	154	33.78
La	1.50	7.84	8.29	6.52	3.12
Ce	5.07	17.74	17.48	14.66	6.98
Pr	0.46	2.27	2.14	2.10	1.24
Nd	2.26	8.91	7.90	8.73	5.96
Sm	0.69	1.83	1.47	2.17	1.87
Eu	0.97	0.57	0.50	0.72	0.64
Tb	1.06	0.24	0.17	2.27	2.43
Gd	2.05	1.63	1.23	0.38	0.42
Dy	11.43	1.46	1.02	2.44	2.85
Ho	3.86	0.30	0.21	0.51	0.62
Er	16.68	0.88	0.62	1.46	1.76
Tm	nd	0.13	0.10	0.22	0.26
Yb	31.76	0.84	0.67	1.38	1.66
Lu	5.44	0.13	0.11	0.21	0.25
Hf	bd	2.37	2.36	2.29	1.20
Ta	3.57	0.17	0.09	0.18	0.08
Pb	101	1.96	6.76	2.79	1.17
Th	3.18	1.80	1.83	2.69	0.58
U	1.10	0.60	0.60	0.53	0.11

Fe_2O_3* = total iron; bd, below detection limit; nd, not determined.
Concentration of trace elements reported in ppm except for Zr to U in the harzburgite, which are in ppb.

Igneous rocks

Bulk rock major and trace-element analyses for four representative samples are given in Table 2. On the basis of lithological relationships and trace-element data, these rocks are divided into two suites: (i) andesite–diorite suite; and (ii) tonalite–diorite suite. These two suites define different fractionation trends on a SiO_2 *vs* FeO*/MgO diagram (Figure 6), with the slope of each trend line suggesting calc-alkaline affinities (Miyashiro 1974). A calc-alkaline nature is also consistent with trace-element interpretations (see below).

Multi-element and REE diagrams normalised to the average N-MORB (Sun & McDonough 1989) for the two suites are presented in Figure 4. Both suites display strong volcanic-arc signatures with high Sr/Nd, U/Nb and Th/Yb ratios and low Ce/Pb, Nb/La and Ti/Eu ratios. These ratios together with LREE enrichments [$(Sm/Nd)_{N\text{-}MORB}$ = 0.51– 0.87] are characteristic of volcanic-arc rocks reflecting either an addition of slab-derived fluids to the mantle

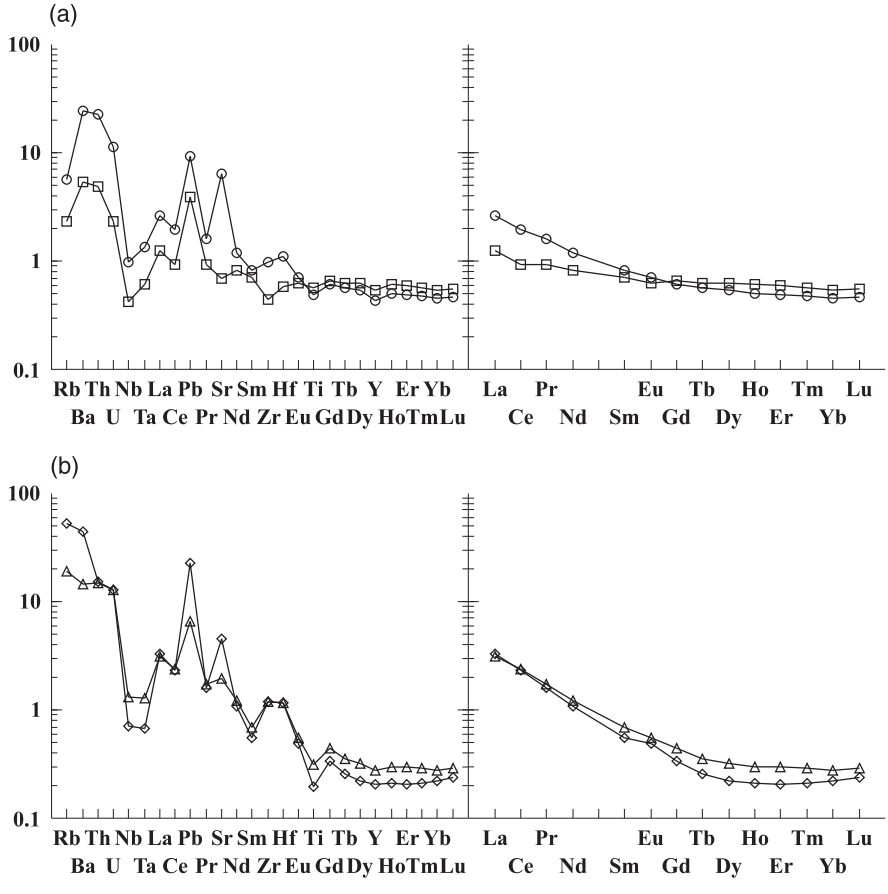

Figure 4 Multi-element (left) and REE (right) diagrams for intermediate lithologies from (a) andesite–diorite (Suite 1); ○, MB78; □, MB79 and (b) diorite–tonalite (Suite 2); △, MB73; ◇, MB74b, normalised to N-MORB values of Sun and McDonough (1989). Note the characteristic arc signatures from both suites and the REE depletion of the diorite–tonalite suite (0.2–0.3 fold N-MORB).

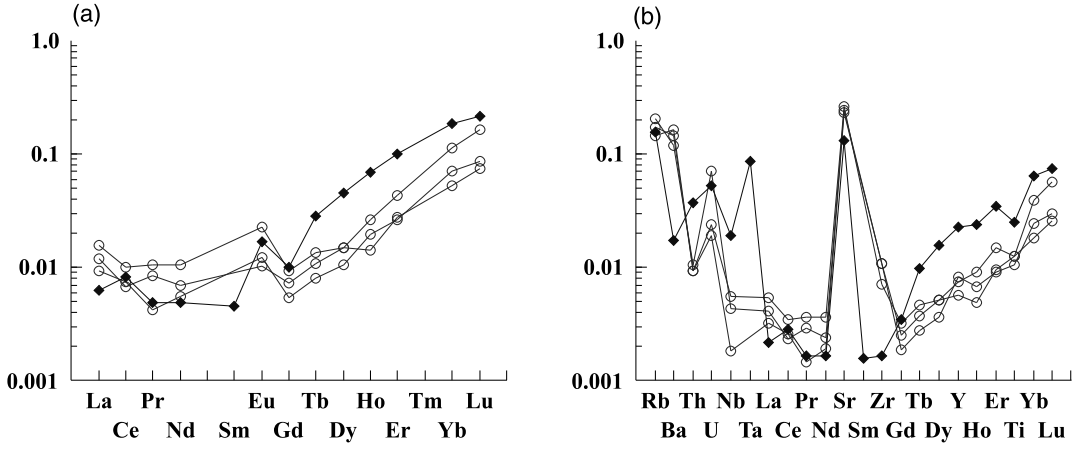

Figure 5 (a) Chondrite-normalised REE plot and (b) primitive-mantle normalised multi-element plot of a South Island harzburgite (MB71a) (◆). The element order is for a strongly depleted harzburgite, which differs from a fertile peridotite (Parkinson & Pearce 1998). The normalisation values for both chondrite and primitive mantle are from Sun and McDonough (1989). Harzburgites from the Torishima Forearc Seamount (Parkinson & Pearce 1998) are plotted for comparison (○).

wedge melting region (Perfit *et al.* 1980; Pearce 1983) or the melting of slightly enriched mantle wedge source with the presence of a high field strength element (HFSE)-bearing residual phase (Morris & Hart 1983; Sun & McDonough 1989). Concentrations of the mobile large ion lithophile (LIL) elements (Cs, Rb, Sr, Ba, Pb and U) could be affected by subsequent metamorphism. However, HFSE (Nb, Ta, Zr, Hf and Ti) and REE (La, Ce, Pr, Nd, Sm, Eu, Gd, Tb, Dy, Ho, Er, Tm, Yb and Lu) are generally considered immobile during low-grade metamorphism (Campbell *et al.* 1984; Lesher *et al.* 1986), except for conditions of high water/rock ratios and carbonate alteration (Humphris 1984), neither of which appear to have been experienced by these rocks. Therefore, the geochemical systematics preserved by HFSE and REE are interpreted to be of primary igneous origin.

Rocks of the tonalite–diorite suite are similar to adakites and high-Al trondhjemite–tonalite–dacite suites as described by Drummond *et al.* (1996). The South Island terrane tonalites are high in Al_2O_3 (> 16%) and low in Y (< 8 ppm), Nb (< 4 ppm) and Yb (< 0.9 ppm). Adakites are believed to result from melting of young (< 25 million years), hot, subducting oceanic crust (quartz eclogite), leaving behind a hornblende- and garnet-rich residue (Drummond & Defant 1990; Drummond *et al.* 1996).

Rocks from both suites plot within the volcanic-arc field on the Th–Hf–Ta diagram of Wood (1980) (Figure 7) and have low Hf/Th ratios < 3, typical of calc-alkaline volcanics.

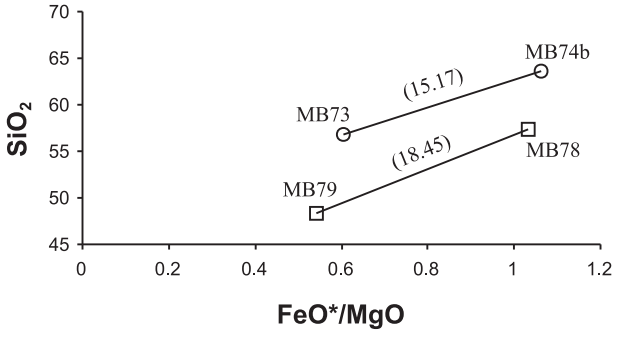

Figure 6 SiO_2 *vs* FeO*/MgO diagram denoting different fractionation trends for the andesite–diorite suite (□, Suite 1) and the diorite–tonalite suite (○, Suite 2). The bracketed number refers to the slope of the 'trend' (note only two points), which according to Miyashiro (1974) depicts both suites as calc-alkaline (i.e. > 6.4). FeO* = total iron reported as FeO.

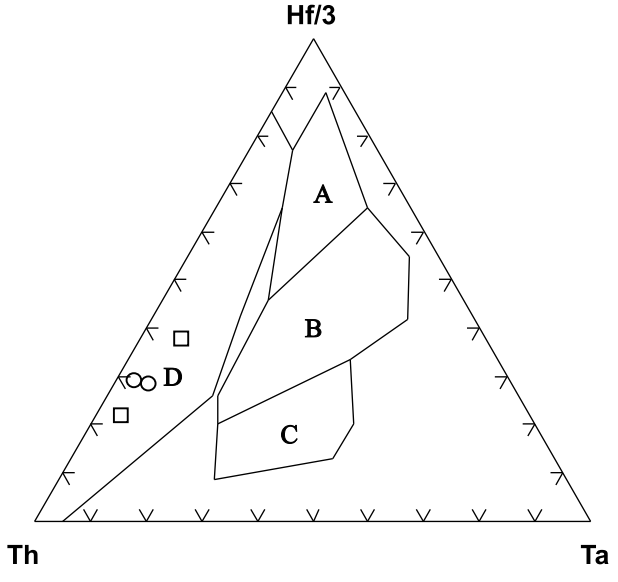

Figure 7 Th–Hf–Ta discrimination diagram of Wood (1980). A, N-MORB; B, E-MORB and within-plate tholeiites and differentiates; C, within-plate basalts and differentiates; D, destructive plate basalts and differentiates. Both suites of the South Island terrane igneous rocks plot in the volcanic-arc field with Hf/Th ratios < 3, typical of calc-alkaline magmatism. □, Suite 1; ○, Suite 2.

GEOCHRONOLOGY

K–Ar analytical details

Argon isotopic composition was determined by isotope dilution using ^{38}Ar as a tracer (Dalrymple & Lanphere 1969).

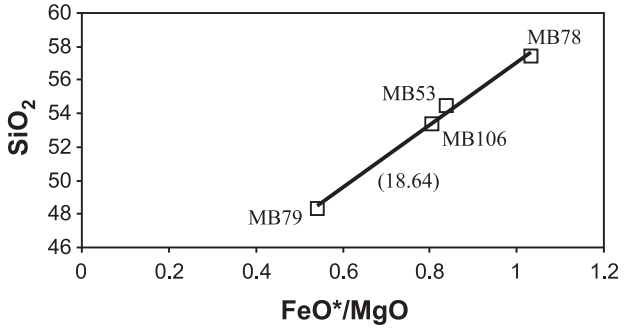

Figure 8 SiO_2 *vs* FeO*/MgO diagram showing a basaltic andesite and a diorite from the V4 calc-alkaline intrusives of the Marlborough ophiolite, Marlborough terrane (MB53, MB106), plotting along the same fractionation trend as that defined by Suite 1 of the South Island terrane (MB78, MB79). Number in brackets depicts the slope of the line (cf. Figure 5).

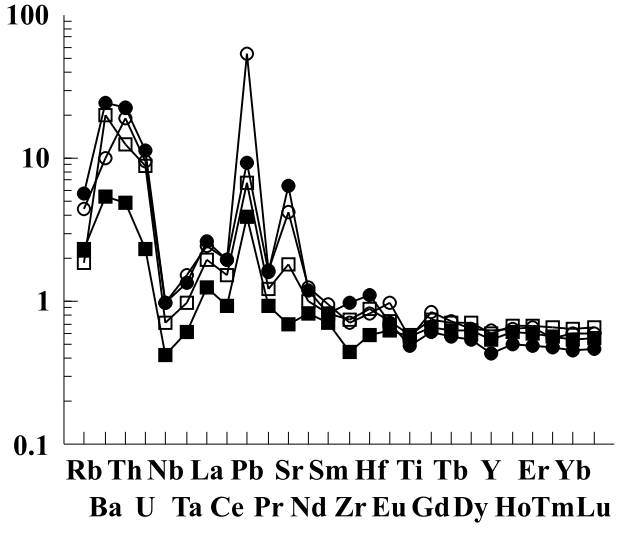

Figure 9 N-MORB (Sun & McDonough 1989) normalised incompatible-multi-element diagram of Suite 1 rocks from the South Island terrane (●, MB78; ■, MB79) and V4 intrusives from the Marlborough terrane (○, MB53; □, MB106). Note the close similarities in patterns.

Samples were fused in a molybdenum crucible under vacuum. The gases were purified by getters and analysed on a VG Gas Analysis 8-80 mass spectrometer at the University of Queensland. The mass spectrometer was operated in static mode at 2 kV accelerating voltage. Ages were calculated from data corrected for machine mass discrimination and system blanks using the decay constants of Steiger and Jäger (1977). The K_2O content of the samples was determined in duplicate by atomic absorption. The quoted errors for the ages are at 1σ and include all uncertainties in the measurement of the isotope ratios and potassium contents (Table 3) (Cox & Dalrymple 1967). Replicate analysis ($n = 13$) of separate loads of the ANU standard biotite have yielded a mean K–Ar age of 97.8 ± 2.1 Ma (cf. 97.9 ± 0.9 Ma: McDougall & Roksandic 1974).

Results

Plagioclase separates from a pillow andesite and amphibole separates from a cumulate amphibole-rich diorite of the Chase Point Meta-andesite record K–Ar dates of 230 ± 10 Ma and 277 ± 7 Ma, respectively. The errors (1σ) result from relatively low abundances of radiogenic ^{40}Ar because of the low K content of the minerals (Table 3). The older age of *ca* 277 Ma (Early Permian) obtained from primary amphibole (magnesio-hastingsite) is interpreted as the crystallisation age for this event. The relatively pristine nature of the magnesio-hastingsite suggests that excess Ar was not a problem. The younger age of *ca* 230 Ma is interpreted to reflect resetting of the respective isotopes during subsequent greenschist-facies metamorphism (300–500°C), an argument supported by the 200–250°C blocking temperature of K–Ar in plagioclase.

Table 3 K–Ar mineral data from lithologies of the South Island terrane.

	Diorite (MB79) Amphibole	Andesite (MB78) Plagioclase
K_2O%	0.205	0.11
^{40}Ar radiogenic (%)	66.92	46.13
^{40}Ar radiogenic (mol g^{-1})	8.82695 × 10–11	3.87895 × 10–11
1σ precision	0.0265	0.0388
Minimum age (Ma)	277 ± 7	230 ± 10
Interpretation	Magmatic age	Metamorphic age

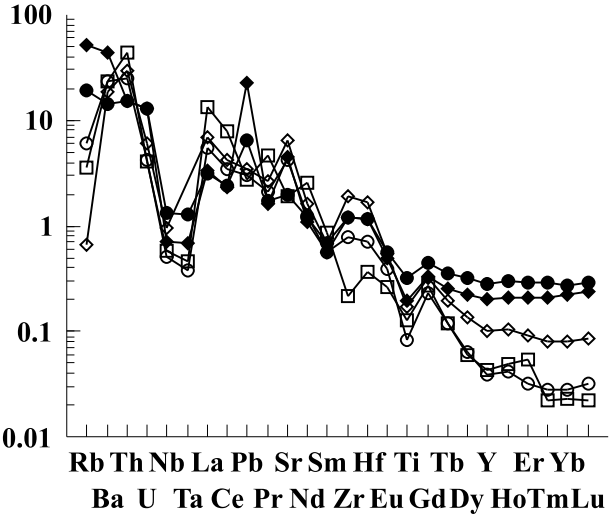

Figure 10 N-MORB (Sun & McDonough 1989) normalised incompatible-multi-element diagram of Suite 2 rocks from the South Island terrane (●, MB73, ◆, MB74b) and V4 trondhjemite–tonalites from the Marlborough terrane (◇, MB63b; □, MB57; ○, MB20). Note the similar patterns. Ta is not plotted for MB63b as it was ludicrously high (contamination?). The variation in heavy-REE concentrations can be explained by crystal fractionation/accumulation (see Figure 11).

OCEANIC ARC OR CONTINENTAL MARGIN?

Igneous rocks from the South Island terrane are dominated by calc-alkaline, intermediate volcanics and granitoids with little evidence of basaltic volcanism. Such an intermediate compositional range may suggest significant crustal involvement in magma generation. However, we cannot rule out the possible genesis in a 'mature' oceanic-arc setting, especially considering their depleted HFSE and HREE concentrations and relatively low-K (low-La) nature. The data overlap the continental-margin-arc and oceanic-arc fields on the Th/Yb *vs* Ta/Yb diagram of Pearce (1983) (not shown). However, this diagram was derived mostly from basalts and is thus not strictly applicable to more differentiated lithologies. Similarly, the Zr/Y *vs* Zr and other diagrams of Pearce (1983) (not shown) for basalts do not apply. The overall incompatible-trace-element systematics of the South Island terrane igneous rocks are consistent with an oceanic-arc environment with HFSE and HREE contents characteristically more depleted than the average N-MORB of Sun and McDonough (1989), suggesting melting from a depleted asthenospheric source. The low K (low La) nature of these igneous rocks is also consistent with this interpretation.

Chromium spinel mineralogy from the serpentinites suggests a supra-subduction zone genesis for the South

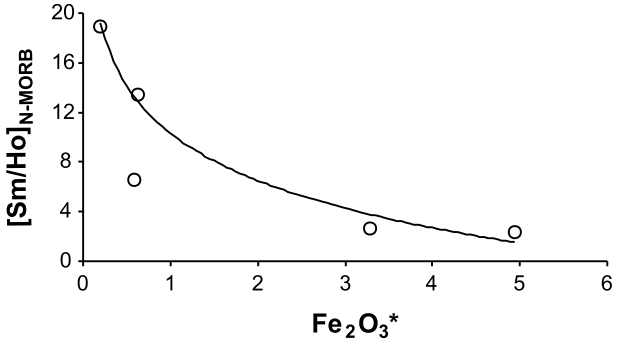

Figure 11 Sm/Ho ratio normalised to N-MORB *vs* Fe_2O_3* diagram. The negative correlation can be explained by the fractionation/accumulation of amphibole and pyroxene, which is consistent with petrographic observations. Sm/Ho is a measure of HREE depletion, which along with Fe_2O_3 concentration, is chiefly controlled by amphibole and pyroxene in these rocks. Note that one sample (MB63b) plots off the main trend. This may be due to iron loss during metamorphism. Fe_2O_3* = total iron.

Island harzburgite, although not necessarily from an island-arc environment. However, the spinels are comparable to spinels from harzburgites of the oceanic Mariana forearc. Chondrite and primitive-mantle normalised incompatible-trace-element plots from the South Island harzburgite are almost identical to harzburgites from the Torishima Seamount from the Izu–Bonin forearc, also suggesting an oceanic-arc origin.

SIMILARITIES TO ROCKS OF THE MARLBOROUGH TERRANE

Leitch *et al*. (1994) correlated rocks of the South Island terrane with units of the Marlborough terrane because it also contains serpentinised ultramafic rocks with associated intrusive and volcanic rocks. The present-day offset of the two terranes was thought to result from a dextral displacement along the Stanage Fault Zone (Leitch *et al*. 1994; Morand 1997). Our new data (this study; Bruce *et al*. 2000) demonstrate that this interpretation is incorrect. Both ultramafic and associated intrusives/volcanic rocks from South Island are young (Early Permian) and have petrological and geochemical characteristics of supra-subduction zone origin, whereas the Marlborough ultramafic and gabbroic rocks are old (Neoproterozoic) and formed at a sea-floor spreading centre (Bruce *et al*. 2000). Clearly, the South Island terrane and the bulk of the Marlborough terrane are unrelated in time, space and origin. However, the Marlborough ultramafic–mafic complex comprises the tectonomagmatic products of four episodes (V1, V2, V3, V4 of Bruce & Niu 2000). The volumetrically insignificant V4 intrusives in the Marlborough terrane do resemble igneous rocks of the South Island terrane. The V4 rocks include basaltic andesite, diorite, trondhjemite and tonalite. Igneous rocks from the V4 episode intrude ultramafic lithologies (V1) of the Marlborough terrane.

Figure 6 shows a differentiation trend based on SiO_2, FeO* and MgO ratios for the andesite–diorite suite from the South Island terrane. Figure 8 is the same diagram with V4 basaltic andesite and diorite from the Marlborough terrane also plotted. These data lie along the same fractionation trend (Figure 8). An incompatible-trace-element plot normalised to N-MORB for samples from both terranes is shown in Figure 9. These trace-element patterns are indistinguishable from one another, suggesting derivation from a common source and by a similar process. Furthermore, the V4 trondhjemite–tonalite suite from the Marlborough terrane is also geochemically very similar to the tonalite–diorite suite from the South Island terrane. Both suites have adakite affinities, with the Marlborough terrane rocks high in Al_2O_3 ($\geq 15\%$) and low in Y (< 3 ppm), Nb (< 3 ppm) and Yb (< 0.3 ppm) (Bruce & Niu 2000). An incompatible-trace-element plot normalised to N-MORB for the plutonic suites from both these terranes is shown in Figure 10. A similar pattern is observed in all samples. The major difference is in the relative concentrations of HREE. This is readily explained by the higher abundances of amphibole and pyroxene in the South Island terrane diorites and tonalites compared to the Marlborough trondhjemites–tonalites because these minerals are the major host of middle- and heavy-REE. This interpretation is also consistent with the negative correlation between $(Sm/Ho)_{N\text{-}MORB}$ and Fe_2O_3* in Figure 11. The only remaining difference between the two suites is thus in LIL element concentrations. But arc-generated magmas can tap a multitude of reservoirs including slab-derived fluids, variably depleted and metasomatised mantle wedge and oceanic crust and sediment from the subducting slab. The differences in LIL element ratios between the two suites may simply result from differences in the respective sources of the various components.

CONCLUSIONS

The Early Permian age (277 ± 7 Ma) for the South Island terrane is very similar to that of the Gympie terrane (270–280 Ma: Sivell & McCulloch 1997) and the Berserker terrane (277 ± 4 Ma; Crouch 1999) of central-eastern Queensland. All three terranes experienced volcanic-arc activity, thus their similar ages and relative proximity suggest a close relationship. Elements of the South Island terrane are here interpreted to have formed above a subduction zone in an oceanic-arc environment. The Gympie terrane comprises both island-arc tholeiites and backarc basalts (Sivell & McCulloch 1997), whereas the Berserker terrane is interpreted to have erupted in a backarc or intra-arc basin setting (Crouch 1999). There is a distinct possibility that these terranes represent different sections both across and along the same oceanic arc(s), perhaps proximal to the continental margin as suggested by shallow-marine units in the Berserker terrane (Crouch 1999). The adakite-like intermediate compositions of the South Island terrane igneous rocks suggests that at the time relatively young (< 25 million years) and hot oceanic crust was subducted (Drummond & Defant 1990).

Lithological and geochemical data support the minor presence of South Island terrane igneous rocks in the Marlborough terrane. These data provide the first direct evidence for any correlation between the two terranes. However, the serpentinised ultramafic rocks from the respective terranes are unrelated. This suggests that although the two terranes may have been in relative proximity to one another during Early Permian times, they were never part of the same assemblage. Their present-day dislocation is presumably due to thrusting in the Hunter–Bowen Orogeny and movement along the Stanage Fault Zone (Murray 1974; Leitch *et al*. 1994; Morand 1997).

ACKNOWLEDGEMENTS

This research was carried out as part of MCB's PhD project and was supported by an ARC grant awarded to Yaoling Niu and Rodney Holcombe. We would like to thank Frank Audsley, Sharyn Price and Alan Greig for conducting the major and trace-element analyses and Kim Baublys and David Theide for K–Ar dating. We are also grateful for the assistance of and discussion with Rodney Holcombe, Terrence Harbort and Darcy Milburn in the field. Constructive reviews by Chris Fergusson and Vince Morand are appreciated with gratitude.

REFERENCES

BLOOMER S. H., TAYLOR B., MACLEOD C. J. *ET AL.* 1995. Early arc volcanism and the ophiolite problem: a perspective from drilling in the western Pacific. *In:* Taylor B. & Natland J. eds. *Active Margins and Marginal Basins of the Western Pacific,* pp. 1–30. American Geophysical Union Geophysical Monograph **88**.

BRUCE M. C. & NIU Y. 2000. Evidence for Palaeozoic magmatism recorded in the Late Neoproterozoic Marlborough ophiolite, New England Fold Belt, central Queensland. *Australian Journal of Earth Sciences* **47**, 1065–1076.

BRUCE M. C., NIU Y., HARBORT T. A. & HOLCOMBE R. J. 2000. Petrological, geochemical and geochronological evidence for a Neoproterozoic ocean basin recorded in the Marlborough terrane of the northern New England Fold Belt. *Australian Journal of Earth Sciences* **47**, 1053–1064.

CAMPBELL I. H., LESHER C. M., COAD P., FRANKLIN J. M., GORTON M. P. & THURSTON P. C. 1984. Rare earth element mobility in alteration pipes below massive sulfide deposits. *Chemical Geology* **45**, 181–202.

COX A. & DALRYMPLE G. B. 1967. Statistical analysis of geomagnetic reversal data and the precision of potassium–argon dating. *Journal of Geophysical Research* **72**, 2603–2614.

CROUCH S. B. S. 1999. Geology, tectonic setting and metallogenesis of the Berserker Subprovince, northern New England Orogen. *Queensland Government Mining Journal* **100**, 6–14.

DALRYMPLE G. B. & LANPHERE M. A. 1969. *Potassium argon dating*. W. H. Freeman, San Francisco.

DICK H. J. B. & BULLEN T. 1984. Chromium spinel as a petrogenetic indicator in abyssal and alpine-type peridotites and spatially associated lavas. *Contributions to Mineralogy and Petrology* **86**, 54–76.

DRUMMOND M. S. & DEFANT M. J. 1990. A model for trondhjemite–tonalite–dacite genesis and crustal growth via slab melting: Archean to modern comparisons. *Journal of Geophysical Research* **95**, 21 503–21 521.

DRUMMOND M. S., DEFANT M. J. & KEPEZHINSKAS P. K. 1996. Petrogenesis of slab-derived trondhjemite–tonalite–dacite/adakite magmas. *Transactions of the Royal Society of Edinburgh: Earth Sciences* **87**, 205–215.

HUMPHRIS S. E. 1984. The mobility of the rare earth elements in the crust. *In:* Henderson P. ed. *Rare Earth Element Geochemistry*, pp. 317–342. Elsevier, Amsterdam.

LEITCH E. C., FERGUSSON C. L., HENDERSON R. A. & MORAND V. J. 1994. Ophiolitic and metamorphic rocks in the Percy Isles and Shoalwater Bay region, New England Fold Belt, central Queensland. *Australian Journal of Earth Sciences* **41**, 571–579.

LESHER C. M., GIBSON H. L. & CAMPBELL I. H. 1986. Composition–volume changes during hydrothermal alteration of andesite at Buttercup Hill, Noranda district, Quebec. *Geochimica et Cosmochimica Acta* **50**, 2693–2705.

MCDOUGALL I. & ROKSANDIC Z. 1974. Total fusion $^{40}Ar/^{39}Ar$ ages using the HIFAR reactor. *Journal of the Geological Society of Australia* **21**, 81–89.

MIYASHIRO A. 1974. Volcanic rock series in island arcs and active continental margins. *American Journal of Science* **274**, 321–355.

MORAND V. J. 1997. Tectonic significance of the Shacks Mylonite Zone and related shear zones, northern New England Fold Belt, Queensland. *In:* Ashley P. M. & Flood P. G. eds. *Tectonics and Metallogenesis of the New England Orogen*, pp. 96–108. Geological Society of Australia Special Publication **19**.

MORRIS J. D. & HART S. R. 1983. Isotopic and incompatible trace element constraints on the genesis of island arc volcanics from Cold Bay and Amak Island, Aleutians, and implications for mantle structure. *Geochimica et Cosmochimica Acta* **47**, 2015–2030.

MURRAY C. G. 1974. Alpine-type ultramafics in the northern part of the Tasman Geosyncline—possible remnants of Palaeozoic ocean floor. *In:* Denmead A. K., Tweedale G. W. & Wilson A. F. eds. *The Tasman Geosyncline—a symposium*, pp. 161–181. Geological Society of Australia, Queensland Division, Brisbane.

NIU Y. & BATIZA R. 1997. Trace element evidence from seamounts for recycled oceanic crust in the Eastern Pacific mantle. *Earth and Planetary Science Letters* **148**, 471–483.

NIU Y. & HÉKINIAN R. 1997. Basaltic liquids and harzburgitic residues in the Garrett Transform: a case study at fast-spreading ridges. *Earth and Planetary Science Letters* **146**, 243–258.

PARKINSON I. J. & PEARCE J. A. 1998. Peridotites from the Izu–Bonin–Mariana forearc (ODP Leg 125): evidence for mantle melting and melt–mantle interaction in a supra-subduction zone setting. *Journal of Petrology* **39**, 1577–1618.

PEARCE J. A. 1983. Role of the sub-continental lithosphere in magma genesis at active continental margins. *In:* Hawkesworth C. J. & Norry M. J. eds. *Continental Basalts and Mantle Xenoliths*, pp. 230–249. Shiva, Nantwich.

PERFIT M. R., GUST D. A., BENCE A. E., ARCULUS R. J. & TAYLOR S. R. 1980. Chemical characteristics of island arc basalts: implications of mantle sources. *In:* Le Maitre R. W. & Cundari A. eds. *Chemical Characterisation of Tectonic Provinces*, pp. 227–256. Chemical Geology **30**.

SIVELL W. J. & MCCULLOCH T. 1997. Geochemistry and Sm–Nd isotope systematics of Early Permian basalts from Gympie Province and fault basins in southeast Queensland: implications for mantle sources in a backarc setting at the Gondwana rim. *In:* Ashley P. M. & Flood P. G. eds. *Tectonics and Metallogenesis of the New England Orogen*, pp. 148–160. Geological Society of Australia Special Publication **19**.

STEIGER R. H. & JÄGER E. 1977. Subcommission on geochronology: convention on the use of decay constants in geochronology and cosmochronology. *Earth and Planetary Science Letters* **36**, 359–362.

SUN S-S. & MCDONOUGH W. F. 1989. Chemical and isotopic systematics of oceanic basalts: implications for mantle composition and processes. *In:* Saunders A. D. & Norry M. J. eds. *Magmatism in Ocean Basins*, pp. 313–345. Geological Society of London Special Publication **42.**

WOOD D. A. 1980. The application of a Th–Hf–Ta diagram to problems for tectonomagmatic classification and to establishing the nature of crustal contamination of basaltic lavas of the British Tertiary volcanic province. *Earth and Planetary Science Letters* **50**, 11–30.

Received 19 November 1999; accepted 29 June 2000

APPENDIX 1: SAMPLE LOCATIONS

Sample	Grid reference
MB71a	GR251912
MB71b	GR251912
MB71c	GR251912
MB73	GR270948
MB74b	GR266947
MB78	GR268953
MB79	GR260939

Coordinates are from the Percy Isles 1:100 000 topographic map (8954).